Geochemistry Geophysics Geosystems G3
AN ELECTRONIC JOURNAL OF THE EARTH SCIENCES
Published by AGU and the Geochemical Society

Article
Volume 9, Number 4
8 April 2008
Q04014, doi:10.1029/2007GC001780
ISSN: 1525-2027

Intrabasement reflections of the Ontong Java Plateau: Implications for plateau construction

Hiroyuki Inoue
Ocean Research Institute, University of Tokyo, 1-15-1 Minamidai, Nakano-ku, Tokyo 164-8639, Japan

Now at INPEX Corporation, 4-1-18 Ebisu, Shibuya-ku, Tokyo 150-0013, Japan (hinoue@inpex.co.jp)

Millard F. Coffin
Ocean Research Institute, University of Tokyo, 1-15-1 Minamidai, Nakano-ku, Tokyo 164-8639, Japan

Now at National Oceanography Centre, Southampton, University of Southampton, Waterfront Campus, European Way, Southampton SO14 3ZH, UK (m.coffin@noc.soton.ac.uk)

Yasuyuki Nakamura
Ocean Research Institute, University of Tokyo, 1-15-1 Minamidai, Nakano-ku, Tokyo 164-8639, Japan (saru@ori.u-tokyo.ac.jp)

Kimihiro Mochizuki
Earthquake Research Institute, University of Tokyo, 1-1-1 Yayoi, Bunkyo-ku, Tokyo 113-0032, Japan (kimi@eri.u-tokyo.ac.jp)

Loren W. Kroenke,
Hawaii Institute of Geophysics and Planetology, School of Ocean and Earth Science and Technology, University of Hawai'i at Manoa, 1680 East-West Road, Honolulu, Hawaii 96822, USA (kroenke@soest.hawaii.edu)

[1] The Early Cretaceous Ontong Java Plateau (OJP) in the western equatorial Pacific, Earth's most voluminous large igneous province (LIP), is characterized by intrabasement seismic reflections. To investigate the nature of such reflections, we have analyzed new and all older multichannel seismic (MCS) reflection data from the OJP using an instantaneous phase velocity analysis technique and synthetic seismograms. Intrabasement reflections are most prevalent on the main OJP, especially on its crest. On MCS data, the reflections (1) are semicontinuous and subparallel to the top of igneous basement; (2) in places, have the opposite phase of seafloor reflections; and (3) have an average frequency of ~20 Hz. We calculate synthetic seismograms using impedance contrasts between massive lava and pillow lava flows obtained from downhole logs at OJP scientific drill sites and show that these lithologies can produce intrabasement reflections similar to those observed in the MCS data. Alternatively, to evaluate the possibility of sediment/sedimentary rock interbeds causing the intrabasement reflections, we use published Early Cretaceous sedimentation rates determined from OJP drill sites and published estimates for the duration of massive OJP volcanism to calculate a range of possible sedimentary interbed thicknesses. The range proves to be below the detection limit of the MCS data. Therefore, we conclude that the intrabasement reflections arise from alternating relatively thin lava flows produced at low effusion rates and relatively thick massive flows generated at high effusion rates, both originating from vents and fissures on the OJP, probably on its crest.

Components: 10,171 words, 9 figures, 1 table.

Keywords: large igneous province; lava flow; Pacific Ocean; reflection seismology; Early Cretaceous; oceanic plateau.

Index Terms: 8137 Tectonophysics: Hotspots, large igneous provinces, and flood basalt volcanism; 3038 Marine Geology and Geophysics: Oceanic plateaus and microcontinents; 8414 Volcanology: Eruption mechanisms and flow emplacement.

Received 5 August 2007; **Revised** 24 December 2007; **Accepted** 29 January 2008; **Published** 8 April 2008.

Inoue, H., M. F. Coffin, Y. Nakamura, K. Mochizuki, and L. W. Kroenke (2008), Intrabasement reflections of the Ontong Java Plateau: Implications for plateau construction, *Geochem. Geophys. Geosyst.*, *9*, Q04014, doi:10.1029/2007GC001780.

1. Introduction

[2] The Ontong Java Plateau in the western equatorial Pacific is Earth's most voluminous LIP (Figure 1), encompassing an area of approximately 1.86×10^6 km^2 [*Coffin and Eldholm*, 1994]. Its maximum crustal thickness exceeds 30 km [*Gladczenko et al.*, 1997; *Miura et al.*, 2004], perhaps attaining 38 km at its crest [*Richardson et al.*, 2000; *Klosko et al.*, 2001; *Gomer and Okal*, 2003], with estimated total volume of 56.7×10^6 km^3 [*Gladczenko et al.*, 1997]. Seven Deep Sea Drilling Project (DSDP) and Ocean Drilling Program (ODP) sites penetrating igneous basement beneath a sedimentary section hundreds of meters thick have yielded pillow and massive basalts (Figure 1), while petrological and geochemical studies of a 3–4 km thick basalt section on Malaita (Solomon Islands) indicate that it is obducted OJP crust [*Petterson et al.*, 1997, 1999; *Petterson*, 2004]. Dating of these igneous rocks from cores and outcrops indicates that most of OJP was emplaced in Early Cretaceous time, ca. ~122 Ma, with minor subsequent volcanism at ~90 Ma and more recently [e.g., *Tarduno et al.*, 1991; *Mahoney et al.*, 1993; *Tejada et al.*, 1996, 2002; *Parkinson et al.*, 2002; *Fitton et al.*, 2004]. These studies, however, are somewhat restricted by a maximum penetration of 217 m into the 30+ km thick volcanic and presumably plutonic igneous basement of the main plateau and a maximum exposure of four km of interpreted upper OJP igneous crust on Malaita Island [*Petterson et al.*, 1997, 1999; *Petterson*, 2004].

[3] We conducted multichannel seismic reflection (MCS) investigations of the OJP in 2005 aboard R/V *Kairei* (KR05-01) of the Japan Agency for Marine-Earth Science and Technology (JAMSTEC) and in 1998 aboard R/V *Hakuho Maru* (KH98-01 Leg 2) of the Ocean Research Institute, University of Tokyo, to investigate the origin and evolution of the OJP. Together, these cruises acquired the first complete north-south and east-west MCS transects of the OJP, which are augmented by a dip profile across the southeastern margin of the OJP (EW95-11) and by ties with DSDP/ODP results (Figure 1).

[4] In this paper we address the stratigraphic and structural development of the OJP through integrated analysis of all existing MCS data and scientific drilling results. Our analyses focus on the nature of the upper few kilometers of OJP's igneous crust, in particular its internal stratigraphy and structure characterized by intrabasement reflections on MCS data. We seek to illuminate the nature of these reflections, to date not penetrated by drilling, as well as identify the region of main volcanic vents and fissures on the OJP, by first applying an instantaneous phase velocity analysis technique [*Tsuji et al.*, 2007] to the MCS data, and then undertaking forward modeling of the intrabasement reflections using synthetic seismograms.

2. Background of This Study

[5] The first intrabasement reflections within submarine LIPs were observed on volcanic passive margins, and hypothesized to represent subaerial lava flows [*Hinz*, 1981; *Mutter et al.*, 1982]. This hypothesis was subsequently confirmed by scientific ocean drilling in the North Atlantic region [*Roberts et al.*, 1984; *Eldholm et al.*, 1987; *Larsen et al.*, 1994; *Planke*, 1994; *Planke and Eldholm*, 1994; *Duncan et al.*, 1996; *Planke and Cambray*, 1998; *Planke and Alvestad*, 1999; *Planke et al.*, 2000]. Intrabasement reflections have also been observed within an oceanic plateau, the Kerguelen Plateau [e.g., *Colwell et al.*, 1988; *Coffin et al.*, 1990; *Schaming and Rotstein*, 1990], and drilling has confirmed that they also represent subaerial lava flows [e.g., *Schlich et al.*, 1989; *Coffin et al.*, 2000; *Frey et al.*, 2000].

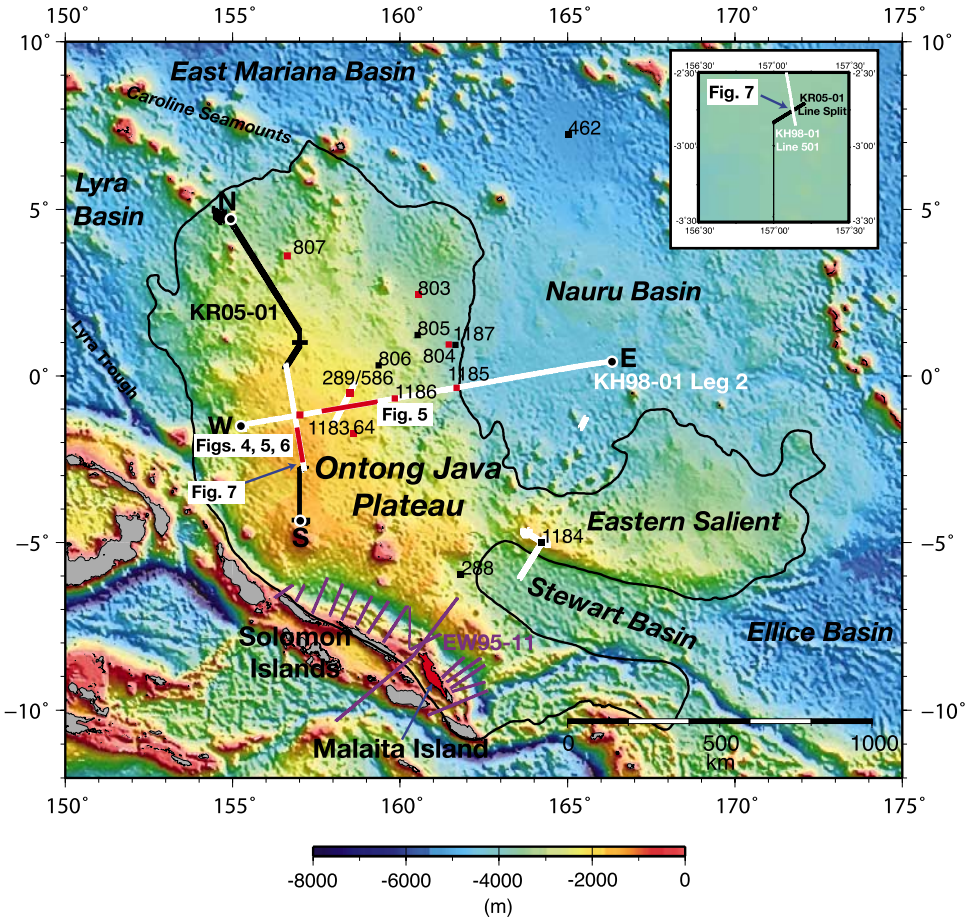

Figure 1. Predicted bathymetry [after *Smith and Sandwell*, 1997] of the Ontong Java Plateau, outlined in black [*Mahoney et al.*, 2001], and surrounding region. Three research cruises have acquired MCS data on the plateau: R/V *Kairei* KR05-01 in 2005 (thick black lines), R/V *Hakuho Maru* KH98-1 Leg 2 (thin white lines) in 1998, and R/V *Maurice Ewing* EW95-11 (thin purple lines) in 1995. Deep Sea Drilling Project (DSDP) and Ocean Drilling Program (ODP) sites on the Ontong Java Plateau and in the Nauru Basin are indicated by squares; those penetrating igneous basement are shown in red. Malaita (Solomon Islands) is indicated in red; other land area appears in gray. Black circles indicate the start and end of composite MCS profiles (Figure 4). Red lines indicate data shown in Figures 5–7. Inset shows zoom-in of intersection of MCS lines KR05-01 Split and KH98-01 Leg 2 501 (see Figure 2 for velocity analysis at the intersection and Figure 7 for MCS data at the intersection).

[6] On the OJP, intrabasement reflections have been observed along its northwestern margin [*Hagen et al.*, 1993], along its southern margin [*Phinney et al.*, 1999, 2004], and on its crest and eastern flank (this paper). What causes the OJP's intrabasement reflections remains enigmatic, however, because unlike lava flows drilled on volcanic passive margins and the Kerguelen Plateau, all lavas drilled on the OJP and sampled in the Solomon Islands were erupted in a submarine environment [e.g., *Michael*, 1999; *Ingle and Coffin*, 2004; *Roberge et al.*, 2005]. Furthermore, no drilling has penetrated these reflections, with the deepest in situ penetration of OJP basement being 217 m at ODP Site 1185 [*Mahoney et al.*, 2001], and correlation between seismic data and field observations of obducted OJP sections in the Solomon Islands is difficult because of limited exposure of the sections.

[7] Early Cretaceous basalts on Malaita Island, termed the Malaita Volcanic Group (MVG), comprise a monotonous sequence of pillow and massive lavas and sills with rare interbedded sediment and sedimentary rock (chert and a quite thin mudstone both calcareous and noncalcareous), and minor microgabbro, gabbro, and dolerite dikes [*Petterson et al.*, 1997, 1999; *Petterson*, 2004]. Rates of lava effusion for obducted OJP basalts on Malaita Island were high to very high [*Petterson et al.*, 1997, 1999; *Petterson*, 2004]. The $^{39}Ar/^{40}Ar$

age of the 0.5 to 3.5 km thick MVG is 123.1 ± 1.4 Ma, and neither the $^{39}Ar/^{40}Ar$ ages nor the volcanic stratigraphy indicate any significant time difference between the lowermost and uppermost lavas [*Tejada et al.*, 2002].

[8] On Malaita Island, individual pillowed and nonpillowed basalt sheets of the MVG vary in thickness between 60 cm and 80 m; about 50% of measured basalt sheets are 5–10 m thick. Pillow diameters or lobe thicknesses vary between 20 cm and 4–6 m, with a modal range of 60 cm to 1 m [*Petterson*, 2004]. At DSDP and ODP sites, thicknesses of sheet basalts vary from several mm to >50 m, but variable core recovery makes statistical analyses difficult [e.g., *Kroenke et al.*, 1991; *Mahoney et al.*, 2001). Downhole logging of two OJP basement drill holes, ODP sites 807C and 1186, indicate massive, dominantly pillowed flows with maximum thicknesses of 28 m [*Kroenke et al.*, 1991] and 7 m [*Mahoney et al.*, 2001], respectively, with thin interbedded sediment and sedimentary rock. Thus, direct observations of the OJP's upper igneous basement stratigraphy and structure are limited to Malaita Island.

[9] Locating the region of OJP's main volcanic vents and fissures has proven problematic, as is even the case for continental flood basalt provinces. Existing single channel seismic (SCS) reflection data from the OJP and adjacent basins do not reveal the location of eruptive centers, including shields [e.g., *Ewing et al.*, 1968; *Kroenke*, 1972; *Erlandson et al.*, 1976; *Hagen et al.*, 1993]. Similarly, DSDP and ODP sites on the OJP have not yielded information on volcanic vents and fissures, nor on associated hydrothermal vents [*Banerjee et al.*, 2004; *Zhao et al.*, 2004]. Studies of continental flood basalts, e.g., Columbia River, suggest that fissure eruptions dominate the major volcanic phase [e.g., *Hooper*, 1997]. The locus of main volcanism has been speculated to have been at the OJP's crest [*Neal et al.*, 1997], which is underlain by a low-velocity mantle root extending to ~300 km depth [*Richardson et al.*, 2000; *Klosko et al.*, 2001; *Gomer and Okal*, 2003].

3. Data Acquisition and Processing

3.1. MCS Data Acquisition and Processing

[10] In 2005, we acquired 1100+ km of two-dimensional MCS data aboard R/V *Kairei* KR05-01, completing a N-S transect of the OJP and Lyra Basin. These data complement 1800+ km of previous MCS data including an E-W transect of the OJP and Nauru basin acquired during R/V *Hakuho Maru* KH98-01 Leg 2 in 1998 (Figure 1).

[11] The KR05-01 MCS data were acquired using a 600 m, 24-trace, 25 m group interval solid streamer, and either one (1500 in^3) or two (main profiles; 2 × 1500 in^3) air guns fired at 20 s intervals, delayed by a random amount between 0 and 1 s [*Stoffa et al.*, 1980]. The KH98-01 Leg 2 MCS data were acquired using a 1200 m, 48-trace, 25 m group interval solid streamer, and between one and four air guns (2 × 1000 in^3 and 2 × 1200 in^3) in various combinations (main profiles are three air guns, 3400 in^3) fired at randomized 20 s intervals. Both data sets were acquired at nonuniform ship speeds resulting in variable shot spacings. CDP intervals for KR05-01 and KH98-01 Leg 2 data were 12.5 and 25 m, respectively. After removing mistimed shots and dead channels, the field data were band-pass (10–75 Hz, with 1–10 Hz and 75–100 Hz tapers) filtered to remove low-frequency cable noise. We used a phase velocity analysis technique that included stacking the amplitude of instantaneous phase (Figure 2), which is sensitive to weak reflections and trace polarity, i.e., poor signal-to-noise ratio intervals [*Tsuji et al.*, 2007]. For these data sets, we performed velocity analyses every 5000 m by defining supergathers from either five successive CMP gathers (KR05-01) or three successive CMP gathers (KH98-01 Leg 2). Following velocity analysis, predictive deconvolution was applied before and after stacking to remove predictable reverberating energy. After stacking, tx (time-distance) and fx (frequency-distance) migration were applied to the KR05-01 and KH98-01 Leg 2 data, respectively. A second band-pass filter and automatic gain control have been applied to all MCS data except synthetic seismograms.

[12] In addition, we reanalyzed a portion of R/V *Maurice Ewing* EW95-11 Line 1 to improve imaging of intrabasement reflections on the OJP. These MCS data extend 160 km from the southernmost OJP to the subduction front at the North Solomon Trench (Figure 1). The streamer length was 3000 m, with receiver group spacing of 25 m. The 20-element, 8510 in^3 air gun array was fired at randomized 20 s intervals, and ship speed was nonuniform [*Phinney et al.*, 1999]. The processing flow was the same as for KH98-01 Leg 2 data.

[13] Our primary processing objective was to image the intrabasement reflections across the entire OJP for the first time. Nevertheless, we did not attempt to enhance these reflections through appli-

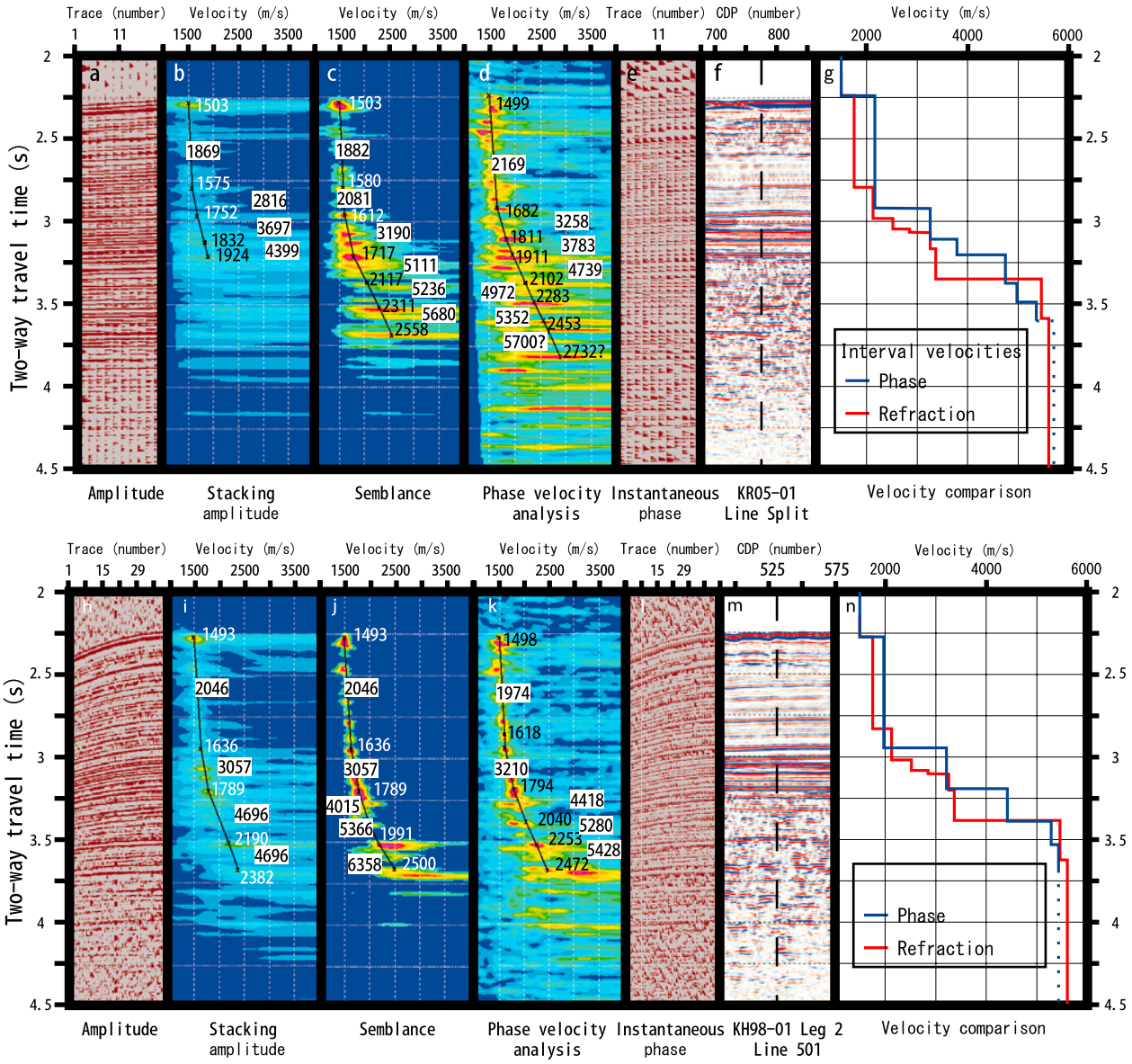

Figure 2. (a–n) Velocity analysis results and comparison of intersecting KR05-01 MCS Line Split (Figures 2a–2f) and KH98-01 MCS Line 501 (Figures 2h–2m) as well as unpublished KH98-01 Leg 2 Line 501 OBS refraction velocities (Figures 2g and 2n). Five (Figure 2a) and three (Figure 2h) common midpoint trace supergather; stacking amplitude contours (Figures 2b and 2i); semblance contours (Figures 2c and 2j); stacking amplitude of instantaneous phase contours (Figures 2d and 2k); common midpoint instantaneous phase trace supergather (Figures 2e and 2l); and MCS line (vertical exaggeration = ~4:1) (Figures 2f and 2m), in which the dashed line indicates the intersection with each MCS Line and the location of the velocity analysis. Crosses indicate locations of velocity picks. Interval velocities are shown in white labels and stacking velocities are shown white and black characters. Figures 2g and 2n compare phase velocities at the intersection (blue) and KH98-01 Leg 2 Line 501 refraction velocities (red) determined from an OBS located 55 km NNW of the intersection. See Figure 7 for longer sections of MCS lines.

cation of specifically tailored gain, or depth- or time-varying filters, to the data.

3.2. Logging Data Processing

[14] Downhole logging data within igneous basement have been acquired from two locations on the OJP, ODP sites 807C and 1186 [*Kroenke et al.*, 1991; *Mahoney et al.*, 2001]. To construct synthetic seismograms, we utilized compressional wave velocities, bulk densities, and formation microscanner (FMS) images obtained from logging. For this purpose, knowledge of the velocity and density

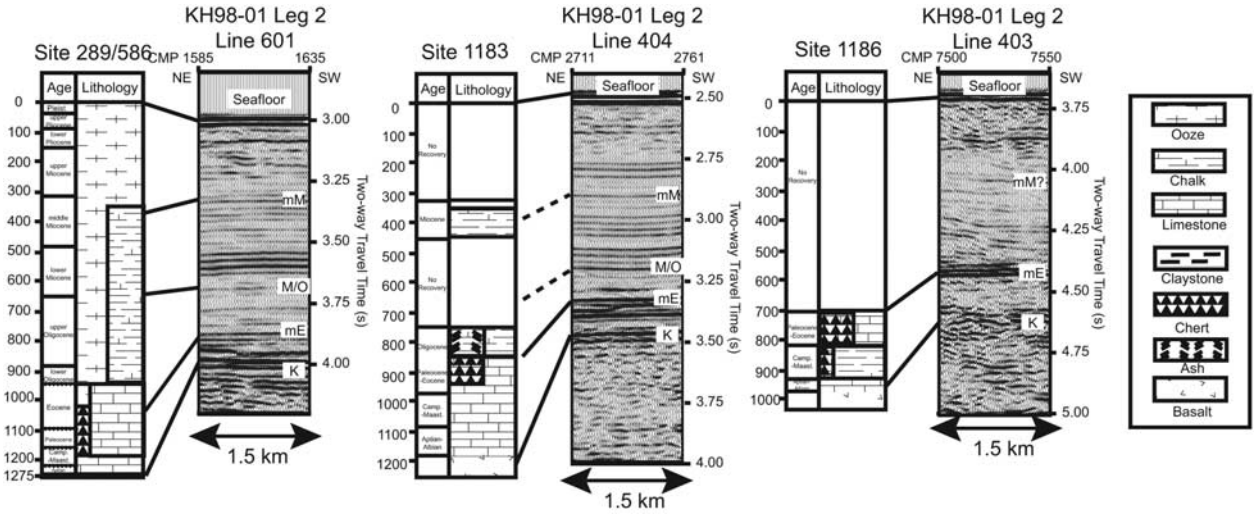

Figure 3. Correlation of DSDP and ODP drilling results with MCS data (vertical exaggeration = ~4:1). The seismic sections are centered on the drill sites. Interpreted ages of reflecting horizons are middle Miocene (mM), Miocene-Oligocene transition (M/O), middle Eocene (mE), and the top of igneous basement (K). Pleist, Pleistocene; Camp, Campanian; Maast, Maastrichtian. See Figure 1 for locations of drill sites and MCS data.

structure in igneous basement is critically important, whereas that of the overlying sedimentary section is important only for estimation of multiple reflections (see section 4.3).

[15] At Site 807, logging data were acquired from two holes, 807A and 807C, although only the latter has FMS data. Although data from both holes have gaps, the sedimentary sections of each hole differ only slightly [*Kroenke et al.*, 1991]. Therefore, we combined data from the two holes to construct synthetic seismograms for the sedimentary section where lines Split and 501 intersect (Figure 1).

[16] At ODP Site 1186, which penetrated 65 m into OJP basement, we used data from high-quality downhole logs of massive (983–989 meters below seafloor, or mbsf) and pillow (970–980 mbsf) basalts to construct synthetic seismograms for igneous basement at the intersection of lines Split and 501 (Figure 1). We interpreted lithofacies from FMS images [*Mahoney et al.*, 2001].

[17] Source wavelets for forward modeling were extracted from MCS data by calculating power spectra. We compared simple stacked seismic data, with no automatic gain control or deconvolution, with these forward models.

4. Data Interpretation and Modeling

4.1. Sedimentary Section of the Main OJP

[18] Correlation of scientific drilling results with MCS data (Figure 3), supplemented by synthetic seismograms and SCS data, enable us to interpret seismic stratigraphy across the OJP (Figure 4). Near the OJP's crest at DSDP Site 289/586 and ODP Site 1183, pelagic drape sediment is interpreted to have been deposited in a low-energy, submarine environment above the calcite compensation depth (CCD) [*Andrews et al.*, 1975; *Kennett et al.*, 1986; *Mahoney et al.*, 2001]. Sediment and sedimentary rock characterized by reflections of low to high amplitude may be divided into three sequences: middle Miocene (mM), Miocene/Oligocene transition (M/O), and middle Eocene (mE) (Figure 3). Similar high-amplitude reflections have been reported elsewhere on the OJP [e.g., *Mosher et al.*, 1993]. At Site 806, near Site 289/586, synthetic seismograms were confined to the upper sedimentary section [*Kroenke et al.*, 1991]. These sequences continue to Site 289/586, and sequence mE has been interpreted at ODP Sites 807, 1183, and 1186. The sequences are laterally continuous and mostly parallel in water depths less than ~2800 m; this relationship is consistent with observations from the northern and northeastern OJP [*Hagen et al.*, 1993; *Mosher et al.*, 1993]. In this region, seafloor topography largely reflects the morphology of the top of basement, despite the sediment and sedimentary rock column being >1000 m thick [*Hagen et al.*, 1993]. This is generally true throughout the study area except around Tauu atoll on the southwestern OJP, a region affected by younger volcanism.

[19] At the transition between the eastern flank of the OJP and the Nauru Basin, the seafloor is rough

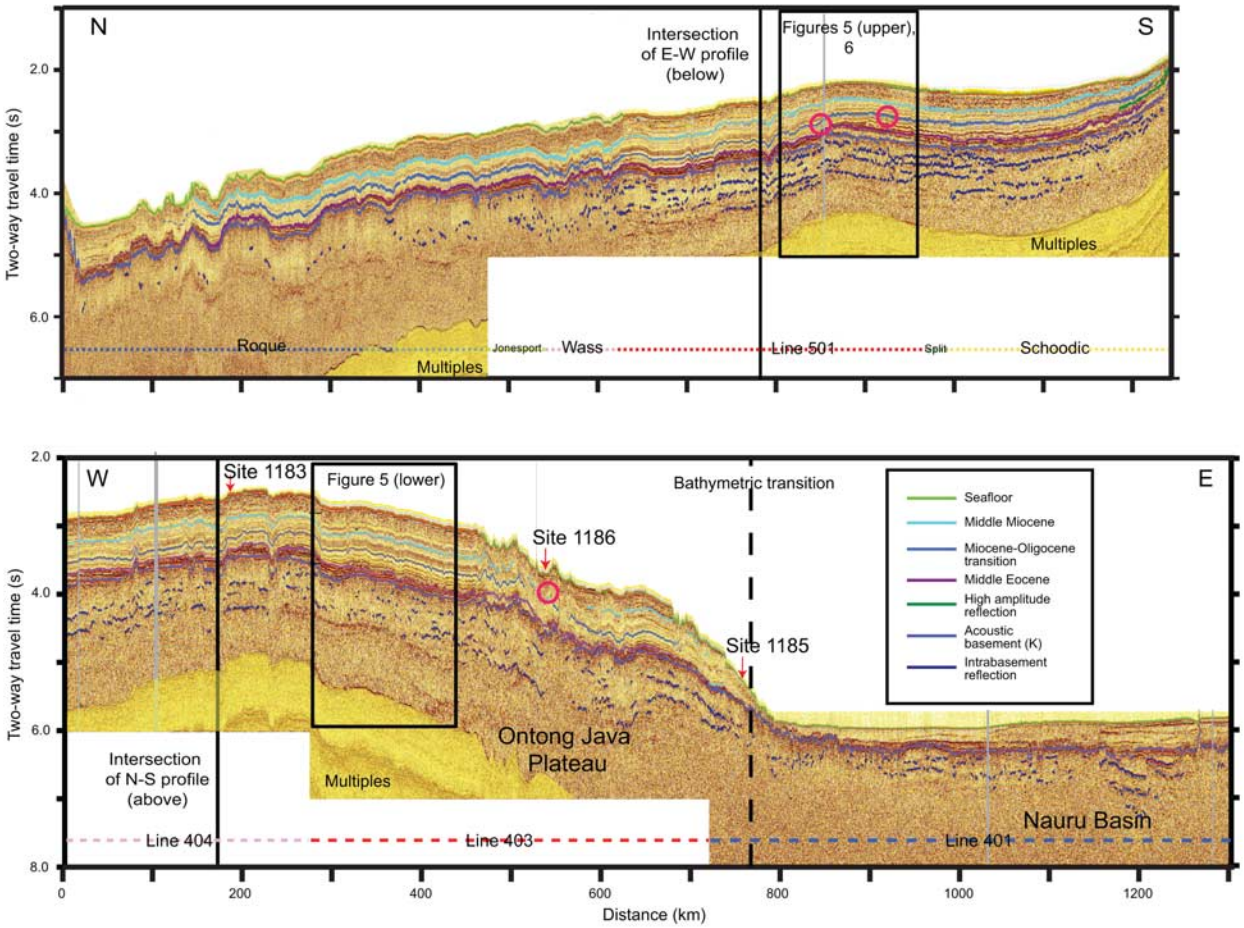

Figure 4. Composite (top) north-south and (bottom) east-west MCS transects of the Ontong Java Plateau, with ages of reflecting horizons (see key) interpreted from drilling results (see Figure 3). Horizontal dashed lines indicate line names, and vertical lines show the intersection of the two transects. Gray zones indicate data gaps. Red circles indicate locations of "eye" structures (see text for discussion). Boxes refer to expanded sections in Figures 5 and 7. See Figure 1 for location. Vertical exaggeration = ~100:1.

and channeled in places, and the sedimentary section contains buried channels as well as evidence for slumps (Figure 4, lower 450–800 km), suggesting a higher-energy sedimentary environment [*Mahoney et al.*, 2001]. In addition, the sedimentary section is deformed by faults not rooted in basement.

[20] The northwestern margin of the main OJP also is characterized by rough seafloor and basement topography, and it is difficult to trace reflections within the sedimentary sequences (Figure 4, upper 0–250 km). The erosional surfaces and irregular basement topography appear to be related to seamounts in this region (e.g., Nukuoro atoll) that could have formed either before or after the main OJP was emplaced [*Hagen et al.*, 1993].

4.2. Igneous Basement, Including Intrabasement Reflections, of the Main OJP

[21] We interpret the high-amplitude reflection K to be the transition between sediment/sedimentary rock and igneous basement (Figures 3 and 4). Beneath K, interval velocities increase to ~5 km/s. This velocity is comparable to compressional wave velocities in igneous basement determined from downhole logging at ODP Site 1186 [*Mahoney et al.*, 2001] and from wide-angle reflection and refraction data [*Furumoto et al.*, 1976; *Hussong et al.*, 1979; *Gladczenko et al.*, 1997]. The uppermost igneous basement consists of pillow and massive lava flows, again with ground truth being the 217 m maximum penetration into OJP's igneous basement, at ODP Site 1185 [*Mahoney et al.*, 2001].

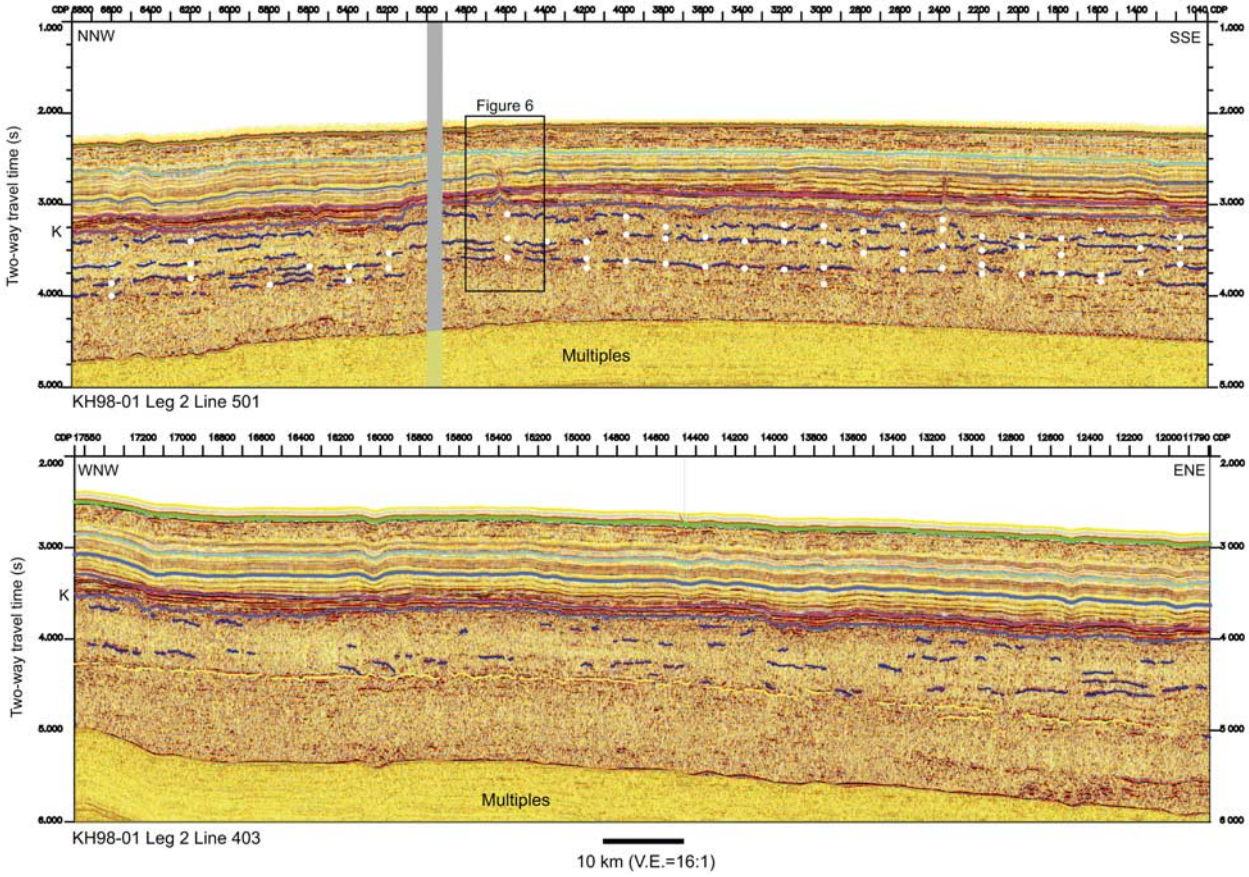

Figure 5. Interpreted KH98-01 Leg 2 MCS lines (top) 501 and (bottom) 403 across the crest of the OJP (see Figures 1 and 4 for location and Figure 4 for key to colors). Reflection "K" (labeled on the left) marks the interface between the sedimentary section and igneous basement. White dots indicate velocity transitions determined from instantaneous phase velocity analysis (see Figure 2). Between the crest and flank of the OJP on line 403 (Figure 5, bottom), laterally continuous, high-amplitude, intrabasement reflections are indicated by yellow lines. Gray zone is a data gap. Note "eye" structures near CDPs 2350 and 4600 on Line 501 (Figure 5, top).

[22] The topography of igneous basement on the main OJP is relatively smooth, suggesting volcanism in a submarine environment. Rarely, we observe distinct volcanic features affecting the sedimentary section. For example, a small (1000 m wide and 500 m high on a single 2-D seismic crossing; true dimensions unknown) knoll on the OJP's northeastern flank (Figure 4, lower ~500 km) probably represents late-stage, postemplacement volcanism. Another example on the MCS data comprises at least three "eye" structures on the main OJP (Figures 4–6) [*Mahoney et al.*, 2001] that resemble hydrothermal vent complexes documented on the Norwegian Vøring and Møre margins [e.g., *Svensen et al.*, 2003, 2004; *Jamtveit et al.*, 2004; *Planke et al.*, 2005]. Such structures, perhaps widespread on the crest of the OJP, probably formed during Oligocene or Miocene time, as interpreted from deformation of the sedimentary section stratigraphically tied to DSDP/ODP drill sites.

[23] Intrabasement reflections are common within the OJP, especially at its crest. These reflections are typically semicontinuous and subparallel (Figures 4–7). Flat horizontal reflections within basement may represent geological interfaces or peg leg multiples; therefore, we undertook instantaneous phase velocity analysis [*Tsuji et al.*, 2007] to discriminate true reflections from multiple energy based on interval velocities. Previous analyses of wide-angle seismic data had not detected these interfaces [*Furumoto et al.*, 1976; *Hussong et al.*, 1979; *Gladczenko et al.*, 1997; *Miura et al.*, 2004; K. Mochizuki, personal communication, 2007]. Intersections of MCS profiles (Figure 7) and accompanying velocity analyses (Figure 2) provide an opportunity to analyze intrabasement reflections in three dimensions. The intrabasement reflections can be correlated on

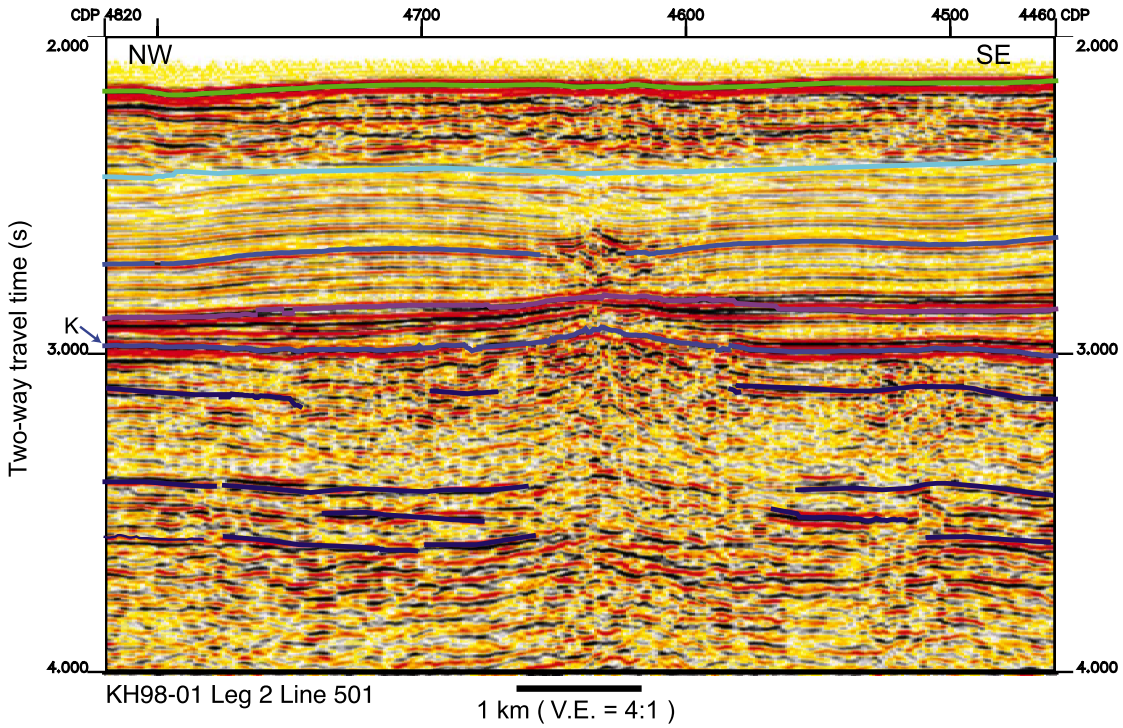

Figure 6. Interpreted KH98-01 Leg 2 MCS Line 501 (see Figures 1 and 4 for location and Figure 4 for key to colors). Reflection "K" (labeled on the left) marks the interface between the sedimentary section and igneous basement. Note the "eye" structure near CDP 4600, which is related to high-amplitude reflections within sediment.

intersecting lines despite different MCS data acquisition parameters, and the interval velocities we have calculated from these reflections fall within the range of OJP upper crustal velocities determined from sonobuoy and ocean bottom seismometer (OBS) data [e.g., *Furumoto et al.*, 1976; *Hussong et al.*, 1979; *Gladczenko et al.*, 1997; *Miura et al.*, 2004] (Figure 2). Because of a strong first seafloor peg leg multiple in the MCS data, our interpretation of intrabasement reflections is restricted to ~1 s two-way travel time (twt), or approximately 2500 m assuming a P wave velocity of 5 km/s, beneath the top of igneous basement at the crest of the OJP (Figure 4).

[24] Using results of our reflection velocity analysis, we reanalyzed unpublished KH98-01 Leg 2 Line 501 OBS data, and we were able to detect minor refractions coinciding with the intrabasement reflections (K. Mochizuki, personal communication, 2007). Refraction velocities from the intrabasement reflections do not differ significantly from reflection velocities. Note that varying reflection velocities of individual intrabasement reflections at the intersection of the two MCS lines probably result from imprecise CDP locations due to nonuniform ship speed. Also, velocities of individual intrabasement reflections are more consistent in the EW95-11 MCS data because of a longer streamer and better tuned air gun source array [*Phinney et al.*, 1999].

[25] Near the crest of the OJP, two or three intrabasement reflections are continuous laterally for 100 km or more (Figures 4, 5, and 7). These reflections lie about 0.2 s (~500 m), 0.5 s (~1400 m), and 0.8 s (~2400 m) in twt below the top of igneous basement at the OJP's crest (Figure 5). On the flanks of the OJP, however, these reflections are not continuous, with observable reflections at the same depth beneath the top of basement separated by tens of kilometer in places (Figures 4 and 5). Between the crest and flank of the OJP, we observe laterally continuous, high-amplitude intrabasement reflections (Figure 5, yellow lines). Despite the resemblance of the intrabasement reflections to multiples, velocity variations can be detected for some of these reflections. However, despite the likelihood that the reflections are not multiples and represent geological interfaces, we have excluded them from consideration herein. Further study of these reflections awaits analysis of coincident KH98-01 Leg 2 sonobuoy and OBS wide-angle data.

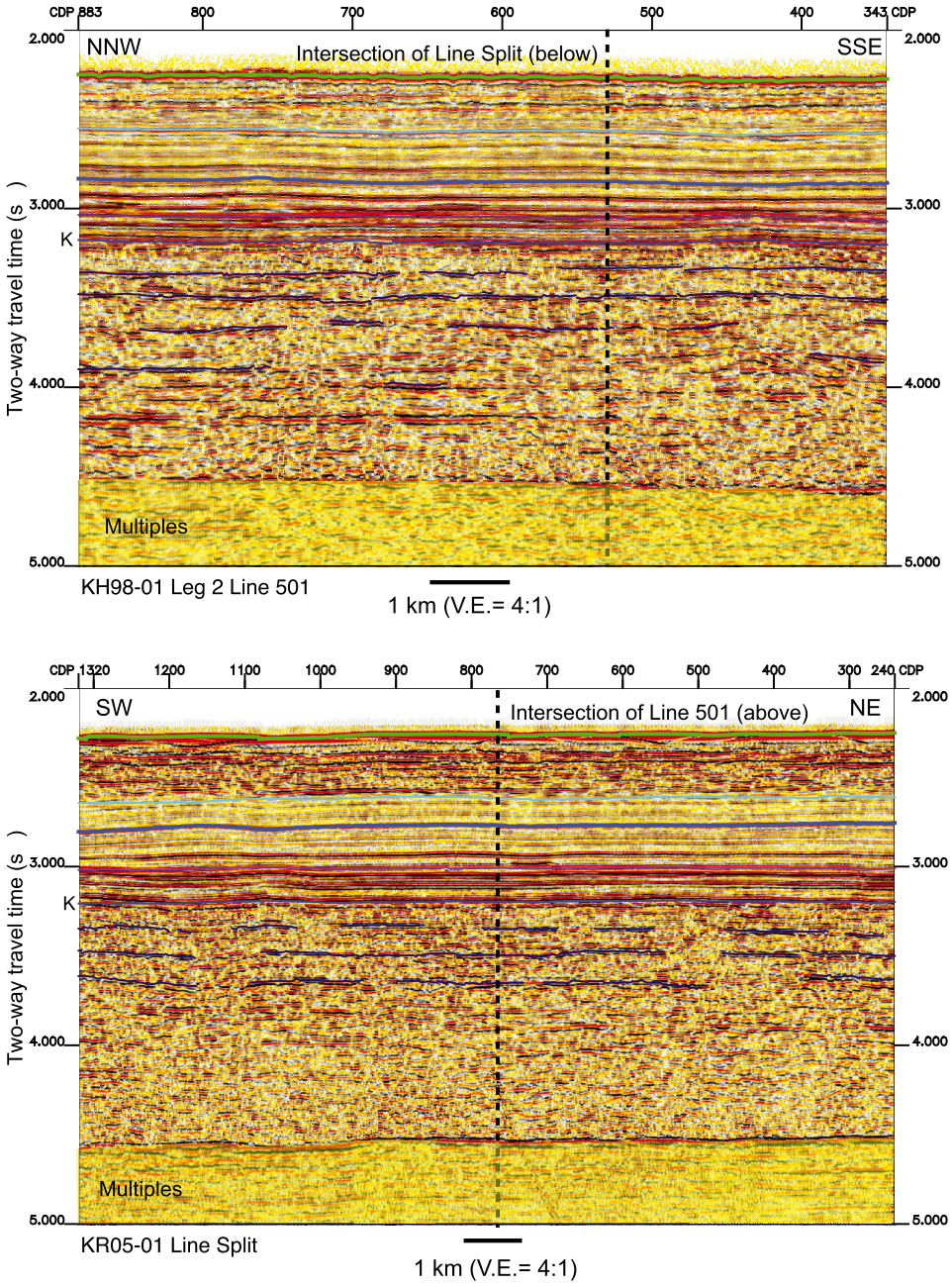

Figure 7. Interpreted (top) KH98-01 Leg 2 Line 501 and (bottom) KR05-01 MCS line Split (see Figures 1 and 4 for location, Figure 2 for velocity analysis, and Figure 4 for key to colors). Reflection "K" (labeled on the left) marks the interface between the sedimentary section and igneous basement. Black dotted lines indicate intersection of the two lines.

[26] Another characteristic of the intrabasement reflections is that some are of opposite phase to seafloor reflections; this is more common near the crest of the OJP than on its flanks (Figure 5). This opposite phase relationship is consistent in near trace offset and simple stacked data, indicating that phases were preserved from the field data. Therefore, we took particular care to preserve phases throughout the data processing flow, e.g., predictive deconvolution.

[27] Last, the average frequency of the intrabasement reflections is ~20 Hz. We calculated this frequency from simple stacked sections, including reprocessed EW95-11 Line 1, which was acquired with a quasi-tuned air gun array.

Table 1. Typical Resolution and Detection Limit Range for Intrabasement Reflections, Based on a Zero Phase Wavelet[a]

Frequency f	Velocity v (m/s) 5000	6000
Wavelength λ (m)		
10 Hz	500	600
20 Hz	250	300
Resolution $\lambda/4$ (m)		
10 Hz	125	150
20 Hz	62.5	75
Resolution $\geq v/2(f_{max}(1 - f_{min}/f_{max}))$[b]		
10–75 Hz (KR05-01 and KH98-01 Leg 2)	38	46
Detectable Limit $1/20\lambda$ $(1/40\lambda)$[c]		
10 Hz	25 (12.5)	30 (15)
20 Hz	12.5 (6.2)	15 (7.5)

[a] For the OJP, a velocity of 5 km/s is representative for both pillow lavas and interbedded chert, and 6 km/s for massive lavas.
[b] *Knapp* [1990].
[c] *Sheriff* [1976].

[28] These results suggest that some intrabasement reflections represent thin low-density and/or low-velocity (negative reflective coefficient) layers within igneous basement. Calculated thicknesses are greater than the detectable limit, but below the limit of vertical resolution (Table 1).

[29] To estimate the effects of a low-density and low-velocity sedimentary layer at the crest of the OJP on MCS data, we used sediment/sedimentary rock ages and sedimentation rates results from ODP Site 1183 [*Mahoney et al.*, 2001], and the duration of main OJP volcanism [e.g., *Tarduno et al.*, 1991; *Mahoney et al.*, 1993; *Tejada et al.*, 1996, 2002; *Parkinson et al.*, 2002; *Fitton et al.*, 2004]. The crest of the OJP was emplaced above the CCD [e.g., *Mahoney et al.*, 2001; *Ingle and Coffin*, 2004; *Roberge et al.*, 2005], although paleodepths on the flanks of the OJP, where previous workers had identified intrabasement reflections, were near or below the CCD [e.g., *Petterson et al.*, 1997, 1999; *Michael*, 1999; *Mahoney et al.*, 2001; *Ingle and Coffin*, 2004; *Petterson*, 2004]. To estimate the thickness of a sedimentary layer within igneous basement, we assumed the Aptian/Albian sedimentation rate of 1.5 m/Ma at ODP Site 1183 (*Sikora and Bergen* [2004], using a basement age of 122 Ma from *Parkinson et al.* [2002]). We also assumed that the duration of main OJP emplacement ranged from a minimum value of 2.8 Ma, assuming that the entire OJP erupted at 123 ± 1.4 Ma, the ^{39}Ar-^{40}Ar age for the 500–3500 m crustal section on Malaita Island [*Tejada et al.*, 2002], to a maximum value of 13 Ma, using biostratigraphic dating results from sediment/sedimentary rock intercalated with lava flow at ODP sites 1186 and 1187, suggesting that magmatism lasted from latest early Aptian time on the plateau crest to late Aptian time on the OJP's eastern edge [*Sikora and Bergen*, 2004]. We consider the ~90 Ma volcanism either to be minor or to result from argon recoil, thereby representing a minimum age [e.g., *Fitton et al.*, 2004]. Therefore, we did not consider the possibility of Late Cretaceous volcanism in these calculations. Thus, from the sedimentation rate of ~1.5 m/Ma and the 2.8–13 Ma range of estimates for OJP emplacement, we calculate that sediment accumulation during main OJP volcanism would have been approximately 4 to 20 m.

[30] This estimated sediment/sedimentary rock thickness is near or less than the detection limit for intrabasement reflections with the seismic sources employed in these MCS data sets, based on a zero phase wavelet (Table 1). Furthermore, the KR05-01 and KH98-01 Leg 2 seismic sources were not tuned, resulting in detection limits higher than those for tuned sources (Table 1). These results suggest that the primary source of intrabasement reflections on the OJP is not sediment or sedimentary rock, but rather volcanic layers of variable acoustic impedance.

4.3. Forward Modeling of Intrabasement Reflections

[31] To estimate the source of intrabasement reflections, our forward modeling approach involved calculating synthetic seismograms for the reflections at ODP Site 1186 and at the intersection of lines Split and 501, using downhole logging data from ODP sites 807 and 1186, in particular density and velocity values of massive and pillow basalts at Site 1186. Three assumptions guided construction of the synthetic seismograms. One, we assumed low impedance volcanic layers. Malaita Island's 3–4 km thick igneous crustal section is dominated by sheets of pillow and massive basalt flows and sills [*Petterson*, 2004]. From field observations on Malaita Island, pillow flows are the sole possible source for negative polarity intrabasement reflections. Intrabasement reflections on the northwestern flank of the OJP have been attributed previously to impedance contrasts between pillows

and massive basalts [*Hagen et al.*, 1993]. Because pillow basalts, massive basalts, and only thin sedimentary interbeds were recovered from DSDP and ODP sites on the main OJP, we assume that pillow lavas are the main cause of negative polarity of the intrabasement reflections. Two, we did not incorporate velocity gradients or compaction effects in the calculations. Igneous basement of the OJP is characterized by significant velocity gradients [e.g., *Gladczenko et al.*, 1997], e.g., the velocity gradient in the ~1 s interval below the top of igneous basement along KH98-01 Leg 2 Line 501 determined from wide-angle OBS data is ~0.5 s^{-1} (K. Mochizuki, unpublished data, 2007). Massive flows, however, are characterized by higher velocities and densities than pillow basalts, as documented by logging data from ODP Site 1186 [*Mahoney et al.*, 2001] as well as from normal oceanic crust at ODP Site 504B [e.g., *Moos et al.*, 1986]. Therefore, we believe that in the uppermost basaltic crust, compaction and velocity gradients are negligible and impedance contrasts between massive and pillow basalts are preserved. Three, we synthesized a sequence of alternating massive and pillow flows, using velocities and densities from one massive and one pillow flow logged at ODP Site 1186 [*Mahoney et al.*, 2001], to construct the synthetic seismograms. Velocities and densities range from 5.5–6.3 km/s and 2.2–2.5 g/cm^3, respectively, for pillow lavas, and 6.9–7.2 km/s and 2.8–3.0 g/cm^3, respectively, for massive lavas. Whereas the cores and crusts of thick, massive subaerial flows have different velocities and densities, and therefore different acoustic impedances [*Planke and Eldholm*, 1994; *Smallwood et al.*, 1998; *Bais et al.*, 2006], little is known about the densities, velocities, and thicknesses of massive submarine flows, hence reliance on results from ODP Site 1186. Note, however, that the velocity and density structure of the massive flow we utilize is similar to that of massive flows cored and logged at ODP Site 504B [*Cann and von Herzen*, 1983].

[32] Our forward modeling results indicate that intrabasement reflections can be generated by relatively low density and velocity pillow lava sequences 30 m thick alternating with relatively high density and velocity massive lava sequences (Figure 8). Low-amplitude reflections are generated by multiple reflections and noise. The different waveshapes for the synthetic and Split MCS data result from attenuation during raypath propagation, interference effects of these layers [*Planke*, 1994; *Planke and Eldholm*, 1994], and a more complex acoustic impedance structure in the OJP than in the model. Our velocity analyses (Figure 2) correlate well with forward modeling results (Figure 8); that is, we picked velocities from reflections at 3.3 s, 3.5 s and 3.7 s twt that are laterally continuous in both MCS data and the synthetic seismograms. In contrast, synthetic seismograms differ from a stack section of the top basement reflection at ODP Site 1186. The differences probably result from tuning effects of high-amplitude reflections associated with chert at 4.3 s twt [*Mahoney et al.*, 2001].

5. Discussion

5.1. Origin of Intrabasement Reflections

[33] Intrabasement reflections have the potential to illuminate important aspects of the OJP's construction. Although intrabasement reflections may have a number of different geological explanations, we propose that alternating massive and pillow flows are dominant cause of intrabasement reflections within the OJP (Figure 9).

[34] The preferred physical volcanological explanation for the origin of the intrabasement reflections is that the uppermost crust of OJP consists of many lava flows, including hyaloclastites several tens of meters thick, erupted at varying effusion rates. High effusion rates produced thicker massive flows extending several hundred kilometers from their vent or fissure sources, and low effusion rates produced thinner pillow flows of lesser or equivalent extent [e.g., *Gregg and Fink*, 1995; *Gregg and Fornari*, 1998]. Thicknesses of individual massive flows may exceed 50 m in LIPs [e.g., *Self et al.*, 1997; *Thordarson and Self*, 1998] including the OJP [*Petterson*, 2004], but our MCS data set did not image shields, vents, or fissures. The maximum mass eruption rate of the 15.1 km^3 Laki

Figure 8. Comparison of forward model synthetic seismograms to seismic reflection data at the intersections of KR05-01 MCS Line Split and KH98-01 MCS Line 501 (see Figures 1 and 4 for location and Figure 2 for velocity analysis). To estimate and incorporate multiple reflections in the modeling, we utilized scaled logging data obtained from ODP Site 807. Source wavelets were extracted from MCS data by calculating power spectra. Lithologic columns (left) represent our geological models. (top) Alternating velocities and densities of pillow and massive basalts, scaled from flows logged at ODP Site 1186, as discussed in the text. (bottom) No velocity or density contrasts in wholly massive basalts.

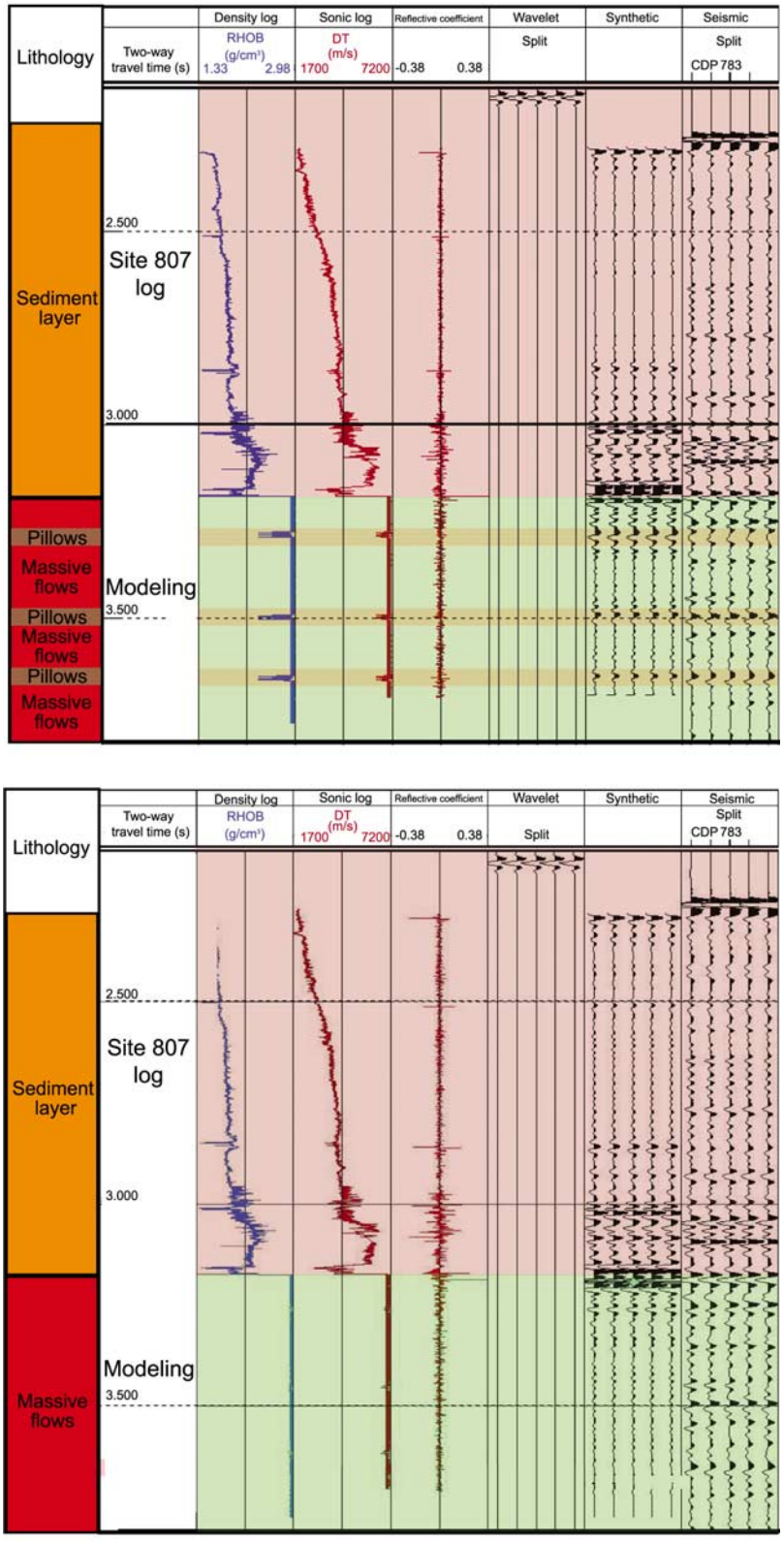
Lithology
Two-way travel time (s)
Density log
RHOB
(g/cm³)
1.33
2.98
Sonic log
DT
(m/s)
1700
7200
Reflective coefficient
-0.38
0.38
Wavelet
Split
Synthetic
Seismic
Split
CDP 783
2.500
3.000
3.500
Site 807 log
Modeling
Sediment layer
Pillows
Massive flows
Pillows
Massive flows
Pillows
Massive flows
Lithology
Two-way travel time (s)
Density log
RHOB
(g/cm³)
Sonic log
DT
(m/s)
1700
7200
Reflective coefficient
-0.38
0.38
Wavelet
Split
Synthetic
Seismic
Split
CDP 783
2.500
3.000
3.500
Site 807 log
Modeling
Sediment layer
Massive flows

Figure 8

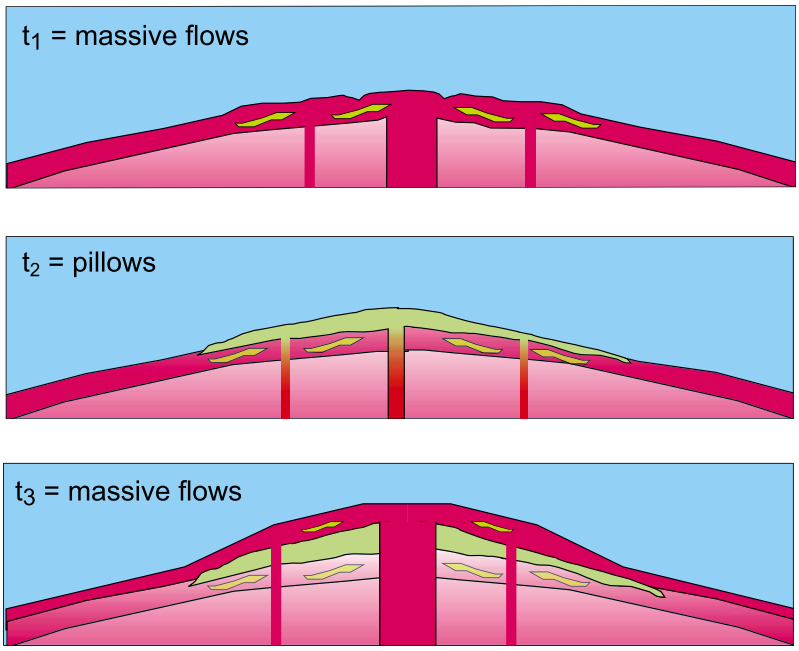

Figure 9. Schematic diagram illustrating volcanic development of OJP's uppermost crust: In the diagram for t_1, high effusion rate of more significant volcanism creates a lava flow unit consisting of multiple thick, laterally continuous, massive flows, each with emplacement durations estimated to be years to decades. In the diagram for t_2, low effusion rate of less significant volcanism creates a lava flow unit consisting of multiple thin, layered, pillow lavas, each with emplacement durations estimated to be days to months. In the diagram for t_3, high effusion rate following low effusion rate creates a lava flow unit consisting of massive flows. Such alternating styles of volcanism result in repetitive layers of massive and pillow lava flow units, which can produce the intrabasement reflections observed in our data (see text for discussion).

flood lava in Iceland in 1783–1784 was ~200 km^3/a; if the ~50 m thick Roza member in the Columbia River flood basalt province were erupted at such a rate, it would have formed in ~10 years [*Thordarson and Self*, 1998]. Such an effusion rate is of the same order of magnitude as the upper end of estimates for the much more poorly dated Ontong Java Plateau, the range for the latter being 10–60 km^3/a [*Coffin and Eldholm*, 1994; *Tejada et al.*, 2002]. Therefore, we believe that it is reasonable to propose that lava flow units representing multiple volcanic events erupted at both high and low effusion rates from vents and fissure on the OJP. In fact, slow spreading mid-ocean ridges are characterized by hummocky structures tens to hundreds of meters high and hundreds to thousands of meters in diameter [e.g., *Head et al.*, 1996]. The forward model synthetic seismograms (Figure 8) suggest such dimensions for piled pillow lavas as the source of intrabasement reflections. Lava flows vary in thickness laterally on Malaita Island [*Petterson*, 2004]; therefore, semi-continuous reflections, as observed in the MCS data, lend credence to our model. Fewer intrabasement reflections on the OJP's flanks may be explained by massive flow cores and thin flow crusts that are below the detection limit of the MCS data, or alternating massive flows and pillow basalts, both of variable thickness, that do not produce high-amplitude reflections. Laterally continuous reflections, however, suggest that low effusion rates prevailed over wide areas of the OJP within specific time intervals, times during which sediment was also likely to have been deposited.

[35] An alternative explanation for the origin of the intrabasement reflections is igneous intrusions. Although the upper crust of the OJP is generally considered to be extrusive [e.g., *Andrews et al.*, 1975; *Hussong et al.*, 1979; *Kroenke et al.*, 1991; *Gladcenko et al.*, 1997; *Mahoney et al.*, 2001], microgabbro intrusions and doleritic sills are found in obducted OJP crust on Malaita Island [*Petterson et al.*, 1997, 1999; *Petterson*, 2004]. Similar igneous intrusions are also found in the Caribbean-Colombian flood basalts [e.g., *Kerr et al.*, 1997]. Intrusive rock should be common near vents and fissures on the OJP. Typical gabbros, however, have velocities of 6.7–6.9 km/s, which are significantly higher than our MCS results (Figure 2) and previous results [*Phinney et al.*, 1999]. Therefore,

we argue that gabbroic intrusions are not likely to be the cause of the intrabasement reflections. On the other hand, dolerite sills are characterized by velocities and densities similar to those calculated and modeled in this study [e.g., *Moberly et al.*, 1986] (Figures 2 and 8), and therefore constitute a plausible cause of the intrabasement reflections. However, semicontinuous intrabasement reflections would imply semicontinuous sills, which may or may not be geologically realistic. Therefore, we regard an intrusive source as unlikely.

[36] Furthermore, we consider other possibilities for the cause of the intrabasement reflections (e.g., widespread volcaniclastic production and distribution during the main OJP eruptive phase, volcanism following the main OJP eruptive phase, and subaerial OJP lava flows) as less viable than the model presented above.

[37] Although volcaniclastic rocks recovered from ODP Site 1184 suggest proximal ~120 Ma subaerial eruptions [e.g., *Thordarson*, 2004; *Chambers et al.*, 2004], thick volcaniclastic rocks have not been identified either on Malaita Island or in DSDP and ODP holes on the main OJP [*Petterson et al.*, 1997, 1999; *Petterson*, 2004]. Geophysical [*Ingle and Coffin*, 2004] and geochemical [*Roberge et al.*, 2005] studies indicate that the main OJP was uplifted to shallower water depths during the main emplacement phase at ~122 Ma, but has never been subaerial. Thus current evidence argues against widespread volcaniclastic rocks as the cause of intrabasement reflections.

[38] Intrabasement reflections on the Kerguelen Plateau [e.g., *Colwell et al.*, 1988; *Coffin et al.*, 1990; *Schaming and Rotstein*, 1990; *Schlich et al.*, 1988; *Coffin et al.*, 2000], volcanic passive margins [e.g., *Hinz*, 1981; *Mutter et al.*, 1982; *Roberts et al.*, 1984; *Eldholm et al.*, 1987; *Larsen et al.*, 1994; *Planke*, 1994; *Planke and Eldholm*, 1994; *Duncan et al.*, 1996; *Planke and Cambray*, 1998; *Planke and Alvestad*, 1999; *Planke et al.*, 2000], and Iceland [e.g., *Smallwood et al.*, 1998] result predominantly from the internal structure of subaerial flows and interbedded sediment/sedimentary rock as well as packets of lavas with similar distributions of thicknesses. A large subaerial sheet lobe typically comprises a vesicular basal zone, a fine-grained lava core, and a vesicular upper crust [e.g., *Self et al.*, 1997; *Thordarson and Self*, 1998]. Seismic reflections are believed to be associated with the impedance contrast between the lava core and basal crust [*Phinney et al.*, 1999], implying that thick lava flows or packets of flows can cause intrabasement reflections. However, whether or not massive submarine lava flows are structured similarly to subaerial flows remains to be tested. In a submarine flow, convective cooling by seawater quenches the outer layer of a flow to glass quickly, and this glass layer acts as an insulating blanket for the lava flow, preventing additional heat loss from the flow interior and allowing a thick submarine flow to advance significantly farther than a similar subaerial flow [*Gregg and Fornari*, 1998]. However, if acoustic impedance contrasts within massive lava flows cause intrabasement reflections on the OJP, it is reasonable to assume that MCS data should image many such reflections, but in the KR05-01, KH98-01 Leg 2, and EW95-11 [*Phinney et al.*, 1999] MCS data, we observe only a limited number of such reflections (Figures 4, 5, and 7).

[39] Yet another hypothesis involves underplating of the OJP at ~90 Ma [e.g., *Ito and Clift*, 1998; *Ito and Taira*, 2000], perhaps caused by the OJP traversing a hot spot [e.g., *Neal et al.*, 1997; *Kroenke et al.*, 2004]. However, a deep crustal transect from the southern OJP to Malaita Island shows little evidence of underplating [*Miura et al.*, 2004], despite the occurrence of intrabasement reflections [*Phinney et al.*, 1999]. If Late Cretaceous or younger volcanism were the cause of the intrabasement reflections within the OJP's upper crust, volcanic rocks postdating the ~122 Ma main emplacement phase should be observed on the main OJP. However, younger basalts are rare on the OJP [e.g., *Fitton et al.*, 2004].

5.2. Location of Main Eruptions of the OJP

[40] Intrabasement reflections interpreted as flows probably mark the main volcanic eruptions constructing the OJP, although no shields, vents, or fissures have been identified on the OJP to date [e.g., *Hagen et al.*, 1993]. We observe intrabasement reflections mainly on the OJP's crest, and they appear to depend on MCS line direction and location (Figures 2 and 5). Near the crest of the OJP, the interpreted volcanic and plutonic crust is >30 km thick [*Gladzcenko et al.*, 1997], and perhaps as thick as 38 km [*Richardson et al.*, 2000; *Klosko et al.*, 2001]. Surface wave tomography has revealed a low-velocity mantle root, probably associated with ~122 Ma volcanism, that appears to extend ~300 km beneath the crest of the OJP [*Richardson et al.*, 2000; *Klosko et al.*, 2001; *Gomer and Okal*, 2003]. These observations suggest the presence of vents and/or fissures on the crest of the OJP. As noted previously, we observe

three "eye" structures probably related to Tertiary volcanic activity, corroborating previous observations of volcanic structures postdating the OJP's main emplacement phase [*Hagen et al.*, 1993].

6. Conclusions

[41] Igneous basement structure and sedimentary sequences are imaged by the first complete north-south and east-west MCS transects of the main OJP. Seafloor topography largely reflects structure of top of basement, and the sedimentary section is continuous in water depths shallower than 3000 m, indicating a low-energy, submarine environment (Figure 2). Along the flanks of the OJP, erosion has affected the sedimentary section and basement topography is irregular in places, both probably associated with submarine canyons and nearby atolls (Figure 4). Basement topography is relatively smooth, and we observe evidence for volcanism or plutonism postdating the main ~122 Ma emplacement phase of the OJP (Figures 5 and 6).

[42] High-amplitude intrabasement reflections enhanced by instantaneous phase velocity analysis are dominantly located in the uppermost few kilometers of igneous crust on the crest of the OJP (Figure 5). These features are semicontinuous and subparallel to basement; some reflections have phase polarities opposite to seafloor reflections; and their average frequency is ~20 Hz. These reflections have not been detected in wide-angle seismic studies, suggesting that they are caused by thin layers above the minimum detection limit, but below the minimum vertical resolution limit, of the seismic sources employed (Table 1). On the basis of sediment deposition rates and the main OJP emplacement duration, the cause of the intrabasement reflections is probably not sediment or sedimentary rock, but rather volcanic layers of variable acoustic impedance. Forward modeling synthetic seismograms of the intrabasement reflections suggest that they are produced by interbedded pillow lavas and massive flows (Figures 8 and 9).

[43] We postulate that the source of the intrabasement reflections is alternating low effusion rate, thinner lava flows, and high effusion rate, thicker massive flows. This model predicts that significant vent and/or fissure eruptions during the main eruptive phase emanated from the crest of the OJP, and we have observed evidence for subsequent volcanic or plutonic activity on the OJP, corroborating previous interpretations [e.g., *Hagen et al.*, 1993].

[44] Although we have advanced our knowledge of igneous basement structure and the region of main volcanic vents and fissures of OJP, we must emphasize that we have employed a limited 2-D MCS data set in investigating a feature the size of Alaska. More detailed geophysical studies, including MCS, combined with deeper drilling, have the potential to greatly increase our understanding of intrabasement reflections on the OJP, as well as to reveal the location of vents and fissures related to the main emplacement phase. Through more work, we hope to gain a more comprehensive understanding of the origin and evolution of the OJP.

Acknowledgments

[45] We thank the masters and crews of R/V *Kairei*, D/V JOIDES *Resolution*, R/V *Hakuho Maru*, and R/V *Maurice Ewing* for their able support of our research. We are grateful for advice and discussions with T. Tsuji on MCS analysis and T. Thordarson on physical volcanology. We greatly appreciate thorough, conscientious, and constructive comments from reviewers A. Harding and S. Self as well as from editor J. Tarduno. This work was supported by grants from the Japan Ministry of Education, Culture, Sports, Science, and Technology (MEXT); the U.S. National Science Foundation (OCE-9714368 and INT-9903454); the Joint Oceanographic Institutions/U.S. Science Support Program; and the Ocean Drilling Program (Legs 192 and 130).

References

Andrews, J. E, et al. (1975), *Initial Reports of the Deep Sea Drilling Project,* vol. 30, 753 pp., U.S. Govt. Print. Off., Washington, D. C.

Bais, G., R. White, M. Worthington, M. Andersen, and SeiFaBa Group (2006), The seismic response of Faroe basalts from integrated borehole and wide-angle seismic data, paper A033 presented at EAGE 68th Conference and Exhibition, Eur. Assoc. of Geosci. and Eng., Vienna, Austria, 12–15 June.

Banerjee, N. R., J. Honnorez, and K. Muehlenbachs (2004), Low-temperature alteration of submarine basalts from the Ontong Java Plateau, in *Origin and Evolution of the Ontong Java Plateau*, edited by J. G. Fitton et al., *Geol. Soc. Spec. Publ.*, *229*, 259–274.

Cann, J. R., and R. P. von Herzen (1983), Downhole logging at Deep Sea Drilling Project sites 501, 504, and 505, near the Costa Rica Rift, *Initial Rep. Deep Sea Drill. Proj.*, *69*, 281–299.

Chambers, L. M., M. S. Pringle, and J. G. Fitton (2004), Phreatomagmatic eruptions on the Ontong Java Plateau: An Aptian $^{40}Ar/^{39}Ar$ age for volcaniclastic rocks at ODP Site 1184, in *Origin and Evolution of the Ontong Java Plateau*, edited by J. G. Fitton et al., *Geol. Soc. Spec. Publ.*, *229*, 325–331.

Coffin, M. F., and O. Eldholm (1994), Large Igneous Provinces: Crustal structure, dimensions, and external consequences, *Rev. Geophys.*, *32*, 1–36.

Coffin, M. F., M. Munschy, J. B. Colwell, R. Schlich, H. L. Davies, and Z. G. Li (1990), Seismic stratigraphy of the

Raggatt Basin, southern Kerguelen Plateau, *Geol. Soc. Am. Bull.*, *102*, 563–579.

Coffin, M. F., et al. (2000), *Proceedings of the Ocean Drilling Program Initial Reports* [CD-ROM], vol. 183, Ocean Drill. Program, College Station, Tex.

Colwell, J. B., M. F. Coffin, C. J. Pigram, H. L. Davies, H. M. J. Stagg, and P. J. Hill (1988), Seismic stratigraphy and evolution of the Raggatt Basin, southern Kerguelen Plateau, *Mar. Pet. Geol.*, *5*, 75–81.

Duncan, R. A, et al. (1996), *Proceedings of the Ocean Drilling Program Initial Reports*, vol. 163, 279 pp., Ocean Drill. Program, College Station, Tex.

Eldholm, O., et al. (1987), *Proceedings of the Ocean Drilling Program Initial Reports*, vol. 104, 783 pp., Ocean Drill. Program, College Station, Tex.

Erlandson, D. L., T. L. Orwig, G. Kiilsgaard, J. H. Mussells, and L. W. Kroenke (1976), Tectonic interpretations of East Caroline and Lyra basins from reflection-profiling investigations, *Geol. Soc. Am. Bull.*, *87*, 453–462.

Ewing, J., M. Ewing, T. Aitken, and W. J. Ludwig (1968), North Pacific sediment layers measured by seismic profiling, in *The Crust and Upper Mantle of the Pacific Area*, *Geophys. Monogr. Ser.*, vol. 12, edited by L. Knopoff et al., pp. 147–173, AGU, Washington, D. C.

Fitton, J. G., J. J. Mahoney, P. J. Wallace, and A. D. Saunders (2004), Origin and evolution of the Ontong Java Plateau: Introduction, in *Origin and Evolution of the Ontong Java Plateau*, edited by J. G. Fitton et al., *Geol. Soc. Spec. Publ.*, *229*, 1–8.

Frey, F. A., et al. (2000), Origin and evolution of a submarine large igneous province: The Kerguelen Plateau and Broken Ridge, southern Indian Ocean, *Earth Planet. Sci. Lett.*, *176*, 73–89.

Furumoto, A. S., J. P. Webb, M. E. Odegard, and D. M. Hussong (1976), Seismic studies on Ontong Java Plateau, 1970, *Tectonophysics*, *34*, 71–90.

Gladczenko, T. P., M. F. Coffin, and O. Eldholm (1997), Crustal structure of the Ontong Java Plateau: Modeling of new gravity and existing seismic data, *J. Geophys. Res.*, *102*, 22,711–22,729.

Gomer, B. M., and E. A. Okal (2003), Multiple-ScS probing of the Ontong-Java Plateau, *Phys. Earth Planet. Inter.*, *138*, 317–331.

Gregg, T. K. P., and J. H. Fink (1995), Quantification of submarine lava-flow morphology through analog experiments, *Geology*, *23*, 73–76.

Gregg, T. K. P., and D. J. Fornari (1998), Long submarine lava flows: Observations and results from numerical modeling, *J. Geophys. Res.*, *103*, 27,517–27,531.

Hagen, R. A., L. A. Mayer, D. C. Mosher, L. W. Kroenke, T. H. Shipley, E. L. Winterer, and W. H. Berger (1993), Basement structure of the northern Ontong Java Plateau, *Proc. Ocean Drill. Program Initial Rep.*, *130*, 23–31.

Head, J. W., L. Wilson, and D. K. Smith (1996), Mid-ocean ridge eruptive vent morphology and substructure: Evidence for dike widths, eruption rates, and evolution of eruptions and axial volcanic ridges, *J. Geophys. Res.*, *101*, 28,265–28,280.

Hinz, K. (1981), A hypothesis on terrestrial catastrophes: Wedges of very thick oceanward dipping layers beneath passive margins—Their origin and paleoenvironment significance, *Geol. Jahrb.*, *E22*, 345–363.

Hooper, P. R. (1997), The Columbia River flood basalt provinces: Current status, in *Large Igneous Provinces: Continental, Oceanic, and Planetary Flood Volcanism*, *Geophys. Monogr. Ser.*, vol. 100, edited by J. J. Mahoney and M. F. Coffin, pp. 1–27, AGU, Washington, D. C.

Hussong, D. M., L. K. Wipperman, and L. W. Kroenke (1979), Crustal structure of the Ontong Java and Manihiki oceanic plateaus, *J. Geophys. Res.*, *84*, 6003–6010.

Ingle, S., and M. F. Coffin (2004), Impact origin for the greater Ontong Java Plateau?, *Earth Planet. Sci. Lett.*, *218*, 123–134.

Ito, G., and P. D. Clift (1998), Subsidence and growth of Pacific Cretaceous plateaus, *Earth Planet. Sci. Lett.*, *161*, 85–100.

Ito, G., and A. Taira (2000), Compensation of the Ontong Java Plateau by surface and subsurface loading, *J. Geophys. Res.*, *105*, 11,171–11,183.

Jamtveit, B., H. Svensen, Y. Y. Podladchikov, and S. Planke (2004), Hydrothermal vent complexes associated with sill intrusions in sedimentary basins, in *Physical Geology of High-Level Magma Systems*, edited by C. Breitkreuz and N. Petford, *Geol. Soc. Spec. Publ.*, *234*, 233–241.

Kennett, J. P., et al. (1986), *Initial Reports of the Deep Sea Drilling Project*, vol. 90, 744 pp., U.S. Govt. Print. Off., Washington, D. C.

Kerr, A. C., J. Tarney, G. F. Marriner, A. Nivia, and A. D. Saunders (1997), The Caribbean-Colombian Cretaceous igneous province: The internal anatomy of an oceanic plateau, in *Large Igneous Provinces: Continental, Oceanic, and Planetary Flood Volcanism*, *Geophys. Monogr. Ser.*, vol. 100, edited by J. J. Mahoney and M. F. Coffin, pp. 45–93, AGU, Washington, D. C.

Klosko, E. R., R. M. Russo, E. A. Okal, and W. P. Richardson (2001), Evidence for a rheologically strong chemical mantle root beneath the Ontong-Java Plateau, *Earth Planet. Sci. Lett.*, *186*, 347–361.

Knapp, R. W. (1990), Vertical resolution of thick beds, thin beds, and thin-bed cyclothems, *Geophysics*, *55*, 1183–1190.

Kroenke, L. W. (1972), Geology of the Ontong Java Plateau, *Tech. Rep. 72-5*, 119 pp., Hawaii Inst. of Geophys., Univ. of Hawaii, Honolulu.

Kroenke, L. W., et al. (1991), *Proceedings of the Ocean Drilling Program Initial Reports*, vol. 130, 1240 pp., Ocean Drill. Program, College Station, Tex.

Kroenke, L. W., P. Wessel, and A. Sterling (2004), Motion of the Ontong Java Plateau in the hotspot frame of reference: 120 Ma to the present, in *Origin and Evolution of the Ontong Java Plateau*, edited by J. G. Fitton et al., *Geol. Soc. Spec. Publ.*, *229*, 9–20.

Larsen, H. C., et al. (1994), *Proceedings of the Ocean Drilling Program Initial Reports*, vol. 152, 977 pp., Ocean Drill. Program, College Station, Tex.

Mahoney, J. J., M. Storey, R. A. Duncan, K. J. Spencer, and M. Pringle (1993), Geochemistry and age of the Ontong Java Plateau, in *The Mesozoic Pacific: Geology, Tectonics, and Volcanism*, *Geophys. Monogr. Ser.*, vol. 77, edited by M. Pringle et al., pp. 233–261, AGU, Washington, D. C.

Mahoney, J. J., et al. (2001), *Proceedings of the Ocean Drilling Program Initial Reports* [CD-ROM], vol. 192, Ocean Drill. Program, College Station, Tex.

Michael, P. J. (1999), Implications for magmatic processes at Ontong Java Plateau from volatile and major element contents of Cretaceous basalt glasses, *Geochem. Geophys. Geosyst.*, *1*(1), doi:10.1029/1999GC000025.

Miura, S., K. Suyehiro, M. Shinohara, N. Takahashi, E. Araki, and A. Taira (2004), Seismological structure and implications of collision between the Ontong Java Plateau and Solomon Island Arc from ocean bottom seismometer-airgun data, *Tectonophysics*, *389*, 191–220.

Moberly, R., et al. (1986), *Initial Reports of the Deep Sea Drilling Project*, vol. 89, 678 pp., U. S. Govt. Print. Off., Washington, D. C.

Moos, D., D. Goldberg, M. A. Hobart, and R. N. Anderson (1986), Elastic wave velocities in layer 2A from full waveform sonic logs at Hole 504B, *Initial Rep. Deep Sea Drill. Proj.*, *92*, 563–570.

Mosher, D. C., L. A. Mayer, T. H. Shipley, E. L. Winterer, R. A. Hagen, J. C. Marsters, F. Bassinot, R. H. Wilkens, M. Lyle, and W. H. Berger (1993), Seismic stratigraphy of the Ontong Java Plateau, *Proc. Ocean Drill. Program Sci. Results*, *130*, 33–49.

Mutter, J., M. Talwani, and P. Stoffa (1982), Origin of seaward-dipping reflectors in oceanic crust off the Norwegian margin by "subaerial seafloor spreading", *Geology*, *10*, 353–357.

Neal, C. R., J. J. Mahoney, L. W. Kroenke, R. A. Duncan, and M. G. Petterson (1997), The Ontong Java Plateau, in *Large Igneous Provinces: Continental, Oceanic, and Planetary Flood Volcanism*, *Geophys. Monogr. Ser.*, vol. 100, edited by J. J. Mahoney and M. F. Coffin, pp. 183–216, AGU, Washington, D. C.

Parkinson, I. J., B. F. Schaefer, and R. J. Arculus (2002), A lower mantle origin for the world's biggest LIP? A high precision Os isotope isochron from Ontong Java Plateau basalts drilled on ODP Leg 192, *Geochim. Cosmochim. Acta*, *66*, A580.

Petterson, M. G. (2004), The geology of north and central Malaita, Solomon Islands: The thickest and most accessible part of the world's largest (Ontong Java) ocean plateau, in *Origin and Evolution of the Ontong Java Plateau*, edited by J. G. Fitton et al., *Geol. Soc. Spec. Publ.*, *229*, 63–82.

Petterson, M. G., C. R. Neal, J. J. Mahoney, L. W. Kroenke, A. D. Saunders, T. L. Babbs, R. A. Duncan, D. Tolia, and B. McGrail (1997), Structure and deformation of north and central Malaita, Solomon Islands: Tectonic implications for the Ontong Java Plateau Solomon arc collision, and for the fate of oceanic plateaus, *Tectonophysics*, *283*, 1–33.

Petterson, M. G., et al. (1999), Geological-tectonic framework of Solomon Islands, SW Pacific: Crustal accretion and growth within an intra-oceanic setting, *Tectonophysics*, *301*, 35–60.

Phinney, E. J., P. Mann, M. F. Coffin, and T. H. Shipley (1999), Sequence stratigraphy, structure, and tectonic history of the southwestern Ontong Java Plateau adjacent to the North Solomon Trench and Solomon Islands arc, *J. Geophys. Res.*, *104*, 20,449–20,466.

Phinney, E. J., P. Mann, M. F. Coffin, and T. H. Shipley (2004), Sequence stratigraphy, structural style, and age of deformation of the Malaita accretionary prism (Solomon Arc-Ontong Java Plateau convergent zone), *Tectonophysics*, *389*, 221–246.

Planke, S. (1994), Geophysical response of flood basalts from analysis of wire line logs: Ocean Drilling Program Site 642, Vøring volcanic margin, *J. Geophys. Res.*, *99*, 9279–9296.

Planke, S., and E. Alvestad (1999), Seismic volcanostratigraphy of the extrusive breakup complexes in the Northeast Atlantic, *Proc. Ocean Drill. Program Sci. Results*, *163*, 1–16.

Planke, S., and H. Cambray (1998), Seismic properties of flood basalts from Hole 917A downhole data, *Proc. Ocean Drill. Program Sci. Results*, *152*, 453–462.

Planke, S., and O. Eldholm (1994), Seismic response and construction of seaward dipping wedges of flood basalts: Vøring volcanic margin, *J. Geophys. Res.*, *99*, 9263–9278.

Planke, S., P. A. Symonds, E. Alvestad, and J. Skogseid (2000), Seismic volcanostratigraphy of large-volume basaltic extrusive complexes on rifted margins, *J. Geophys. Res.*, *105*, 19,335–19,351.

Planke, S., T. E. Rasmussen, S. S. Rey, and R. Myklebust (2005), Seismic characteristics and distribution of volcanic intrusions and hydrothermal vent complexes in the Vøring and Møre basins, in *Petroleum Geology: North-West Europe and Global Perspectives—Proceedings of the* 6th *Petroleum Geology Conference*, edited by A. G. Doré and B. Vining, pp. 1–12, Geol. Soc., London.

Richardson, W. P., E. A. Okal, and S. van der Lee (2000), Rayleigh-wave tomography of the Ontong-Java Plateau, *Phys. Earth Planet. Inter.*, *118*, 29–51.

Roberge, J., P. J. Wallace, R. V. White, and M. F. Coffin (2005), Anomalous uplift and subsidence of the Ontong Java Plateau inferred from CO_2 contents of submarine basaltic glasses, *Geology*, *33*, 501–504.

Roberts, D. G., J. Backman, A. C. Morton, J. W. Murray, and J. B. Keene (1984), Evolution of volcanic rifted margins: Synthesis of Leg 81 results on the west margin of Rockall Plateau, *Initial Rep. Deep Sea Drill. Proj.*, *81*, 883–911.

Schaming, M., and Y. Rotstein (1990), Basement reflectors in the Kerguelen Plateau, south Indian Ocean—Indications for the structure and early history of the Plateau, *Geol. Soc. Am. Bull.*, *102*, 580–592.

Schlich, R., S. W. Wise Jr., and A. A. Palmer (1989), *Proceedings of the Ocean Drilling Program Initial Reports*, vol. 120, 648 pp., Ocean Drill. Program, College Station, Tex.

Self, S., T. Thordarson, and L. Keszthelyi (1997), Emplacement of continental flood basalt lava flows, in *Large Igneous Provinces: Continental, Oceanic, and Planetary Flood Volcanism*, *Geophys. Monogr. Ser.*, vol. 100, edited by J. J. Mahoney and M. F. Coffin, pp. 381–410, AGU, Washington, D. C.

Sheriff, R. E. (1976), Inferring stratigraphy from seismic data, *AAPG Bull.*, *60*, 528–542.

Sikora, P. J., and J. A. Bergen (2004), Cretaceous planktonic foraminiferal and nannofossil biostratigraphy of Ontong Jave Plateau sites from DSDP Leg 30 and ODP Leg 192, in *Origin and Evolution of the Ontong Java Plateau*, edited by J. G. Fitton et al., *Geol. Soc. Spec. Publ.*, *229*, 83–111.

Smallwood, J. R., R. S. White, and R. K. Staples (1998), Deep crustal reflectors under Reydarfjördur, eastern Iceland: Crustal accretion above the Iceland mantle plume, *Geophys. J. Int.*, *134*, 277–290.

Smith, W. H. F., and D. T. Sandwell (1997), Global sea floor topography from satellite altimetry and ship depth soundings, *Science*, *277*, 1956–1962.

Stoffa, P. L., P. Buhl, T. J. Herron, T. K. Kan, and W. J. Ludwig (1980), Mantle reflections beneath the crestal zone of the East Pacific Rise from multi-channel seismic data, *Mar. Geol.*, *35*, 83–97.

Svensen, H., S. Planke, B. Jamtveit, and T. Pedersen (2003), Seep carbonate formation controlled by hydrothermal vent complexes: A case study from the Voring Basin, the Norwegian Sea, *Geo Mar. Lett.*, *23*, 351–358.

Svensen, H., S. Planke, A. Malthe-Sorenssen, B. Jamtveit, R. Myklebust, T. R. Eidem, and S. S. Rey (2004), Release of methane from a volcanic basin as a mechanism for initial Eocene global warming, *Nature*, *429*, 542–545.

Tarduno, J. A., W. V. Sliter, L. Kroenke, M. Leckie, H. Mayer, J. J. Mahoney, R. Musgrave, M. Storey, and E. L. Winterer (1991), Rapid formation of Ontong Java Plateau by Aptian mantle plume volcanism, *Science*, *254*, 399–403.

Tejada, M. L. G., J. J. Mahoney, R. A. Duncan, and M. P. Hawkins (1996), Age and geochemistry of basement and alkalic rocks of Malaita and Santa Isabel, Solomon Islands,

southern margin of Ontong Java plateau, *J. Petrol.*, *37*, 361–394.

Tejada, M. L. G., J. J. Mahoney, C. R. Neal, R. A. Duncan, and M. G. Petterson (2002), Basement geochemistry and geochronology of central Malaita, Solomon islands, with implications for the origin and evolution of the Ontong Java Plateau, *J. Petrol.*, *43*, 449–484.

Thordarson, T. (2004), Accretionary-lapilli-bearing pyroclastic rocks at ODP Leg 192 Site 1184: A record of subaerial phreatomagmatic eruptions on the Ontong Java Plateau, in *Origin and Evolution of the Ontong Java Plateau*, edited by J. G. Fitton et al., *Geol. Soc. Spec. Publ.*, *229*, 239–257.

Thordarson, T., and S. Self (1998), The Roza Member, Columbia River Basalt Group: A gigantic pahoehoe lava flow field formed by endogenous processes?, *J. Geophys. Res.*, *103*, 27,411–27,445.

Tsuji, T., Y. Nakamura, H. Tokuyama, M. F. Coffin, and K. Koda (2007), Oceanic crust and Moho of the Pacific plate in the eastern Ogasawara Plateau region, *Island Arc*, *16*, 361–373.

Zhao, X., M. J. Antretter, L. W. Kroenke, P. Riisager, and S. A. Hall (2004), Relationships between physical properties and alteration in basement rocks from the Ontong Java Plateau, *Proc. Ocean Drill. Program Sci. Results*, 192.